

Modelling tipping-point phenomena of scientific coauthorship networks

Zheng Xie · Enming Dong · Dongyun Yi · Ouyang Zhenzheng · Jianping Li

Received: date / Accepted: date

Abstract In a range of scientific coauthorship networks, tipping points are detected in degree distributions, correlations between degrees and local clustering coefficients, etc. The existence of those tipping points could be treated as a result of the diversity of collaboration behaviours in scientific field. A growing geometric hypergraph built on a cluster of concentric circles is proposed to model two typical collaboration behaviours, namely the behaviour of leaders and that of other members in research teams. The model successfully predicts the tipping points, as well as many common features of coauthorship networks. For example, it realizes a process of deriving the complex “scale-free” property from the simple “yes/no” experiments. Moreover, it gives a reasonable explanation for the emergence of tipping points by the difference of collaboration behaviours between leaders and other members, which emerges in the evolution of research teams. The evolution synthetically addresses typical factors of generating collaborations, such as academic impacts, the homophily of authors, and the communications between research teams, etc.

Keywords Coauthorship network · Hypergraph · Geometric graph · Modelling

Z. Xie

College of Science, National University of Defense Technology, Changsha, 410073, China

E-mail: xiezheng81@nudt.edu.cn

E. Dong

College of Science, National University of Defense Technology, Changsha, 410073, China

E-mail: dongenming@gmail.com

The first two authors contributed equally to this work.

D. Yi

College of Science, National University of Defense Technology, Changsha, 410073, China

Z. Ouyang

College of Science, National University of Defense Technology, Changsha, 410073, China

J. Li

College of Science, National University of Defense Technology, Changsha, 410073, China

1 Introduction

Coauthorship networks express collaborations graphically with nodes representing authors, and links representing coauthor relationships. Since modern sciences increasingly involve collaborative research, the study of coauthorship networks has become an important topic of social science, especially of scientometrics [1], which helps to understand the evolution and dynamics of scientific activities, predict scientific success, etc [2–4]. The empirically observed coauthorship networks have some common local (degree assortativity, high clustering) and global (power-law degree distribution, short average distance) properties [5–8], according to which they are marked as scale-free and small-world networks. Some important models have been proposed to reproduce those properties, such as modeling the scale-free property by preferential attachment [9–15] or cumulative advantage [16], modeling the degree assortativity by connecting two non-connected nodes with similar degrees [17].

One explanation of the power-law tails of degree distributions is inhomogeneous influences of nodes, which means that nodes with wider influences are likely to gain more connections. A good example is that authors with large academic impacts, which are usually small parts in coauthorship networks, possess many collaborators. When using geometric graph theory (RGG) [19, 20] to analyze networks, such as citation networks, web-graphs, the impacts of nodes in academic research or Internet can be modeled by attaching certain specific geometric zones to nodes [21–23]. Likewise our previous geometric graph model for coauthorship networks [24], which is built on a circle and reproduces the aforementioned features of coauthorship networks at certain levels.

Besides the academic impacts, the homophily of authors in the sense of geographical distances and research interests is another factor of generating collaborations [25]. Comparing with topological graph models, an advantage of our model in Ref [24] is that it models the homophily by spatial coordinates of nodes. However, in that model, authors are generated at one time, so it can not express the formation process of coauthorship networks. A growing geometric hypergraph is proposed here to model this process. It is built on a cluster of concentric circles, where each circle has a time coordinate.

Unlike our previous model, the new model imitates the collaborations in and between research teams in dynamic ways. The main collaborations occur in the same research team, which synthetically represent the influences of the homophily as well as the academic impacts of authors and the ageing of those impacts (which is not considered in our previous model) on collaborations in geometrical ways. Our analysis shows that the model can also capture the aforementioned features of the empirical data.

Interesting phenomena of the empirical data are the tripping points emerged in degree distributions $P(k)$, average local clustering coefficient and average degree of neighbors as functions of degrees ($C(k)$, $N(k)$). The data features are different in the two regions of k splitted by tripping points, e.g. $P(k)$ emerges generalized Poisson and power-law respectively. Our model successfully reproduces the shapes of those functions (much better than our previous

model [24]) as well as their tipping points, and gives reasonable explanations for the tipping-point transitions.

The components of authors with large degrees are analyzed. The members of large “article team”s [16] are large degree authors. Each such team is a set of researchers appeared as authors in an article. It is found that when removing large article teams, the degree distributions still have a power-law tail. Our model provides a reasonable explanation for the finding: the power-law tails are caused by the articles with many authors as well as the leaders of large research teams.

This report is organized as follows: the model and data are described in Sections 2 and 3 respectively; the degree distribution, clustering, and assortativity of the modeled networks are analyzed in Sections 4 and 5 respectively; and the conclusion is drawn in Section 6.

2 The model

In reality, although there exist some researchers who do scientific research alone, most researchers belong to some research teams in universities or research institutes. In each research team, one or several professional researchers can be treated as leaders. So “research teams” and their “leaders” are considered in our model, which have been used in Ref [24]. The term of “article team” in Ref [16] is also adopted by the model. Our model creates “authors” (nodes) by a unit intensity Poisson process in batches, and randomly selects some of the nodes as “leaders” to attach specific geometric zones imitating their academic impacts. For each leader, a research team can be formed consisting of the leader and researchers within his impact (Fig 1). Different from the “lead author” who in charge of an “article team” in S. Milojević’s model [16], the leaders in our model are in charge of research teams, and concurrently play the roles of lead authors of article teams.

Inspired by the processes of generating coauthorship networks, the model generates hypergraphs first (in which authors are regarded as nodes and article teams as hyperedges), then extracts simple graphs from the hypergraphs (in which edges are formed between every two nodes in each hyperedge). Note that the isolated nodes are ignored and the multiple edges are treated as one.

Coauthorship networks can evolve over time. Many new articles are published per week or month. Consequently, the number of hyperedges and nodes in the model are growing with time, driven by a time parameter t , which can be explained as the t -th unit of time, such as t -th week, t -th month, etc. Our model is designed to simulate the evolution process of coauthorship networks. The way of generating hyperedges of new nodes is different from that of our previous model [24], i. e. a new node will coauthor with its leaders and some existing research team members nearest to it. So, in the end, the authors (who could be non-leaders) with high scientific ages can write articles together with the authors who are not their nearest neighbors, since the nearest neighbors may not be generated when the articles were written. This difference causes

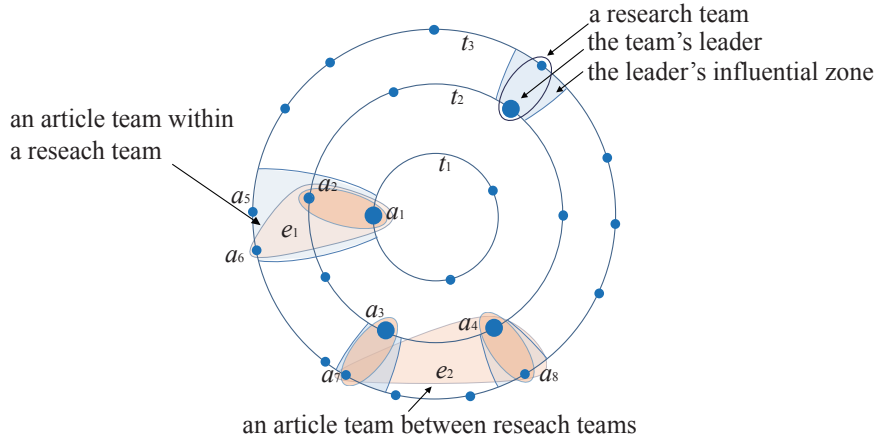


Fig. 1 Illustration of the model. The leaders (large nodes) have zones representing their academic impacts, the sizes of which changes over time. The set of the nodes in a zone (blue area) is regarded as a research team, and the set of the nodes in a hyperedge (red area) as an article team. The sizes of research teams are expressed by geometric sizes.

the diversity of scientific ages not only for leaders (which is considered in the model in Ref [24]), but also for non-leaders. An illustration is shown in Fig 1. When the new author a_6 at time t_3 writes an article (which has three authors), it should coauthor with its leader a_1 and one nearest existing nodes in the research team of a_1 , namely a_2 , but not the nearest one a_5 .

The hypergraph model aims at simulating the self-organizing formation mechanisms of coauthorship networks. The expected sizes of hyperedges are drawn from a mixture distribution of generalized Poisson and power-law (Fig 2). The probability density function (PDF) of such kind of distribution is formulated by $f(x) = qf_1(x) + (1 - q)f_2(x)$, where $f_1(x) = a(a + bx)^{x-1}e^{-a-bx}/x!$ and $f_2(x) = cx^d$ are the PDFs of the distributions of generalized Poisson and power-law respectively, $a, b, x \in \mathbb{R}^+$, $c, d \in \mathbb{R}$ and $q \in [0, 1]$. Note that the size distribution of hyperedges is an output in the model of S. Milojević [16] (in which the distribution is treated as a mixture of exponential and power-law), but is an input here.

Based on the assumptions above, a modeled hypergraph built on a cluster of concentric circles S_t^1 , $t = 1, \dots, T$, is generated as follows:

1. Coordinate and influential zone (simply ‘zone’ hereafter) assignment

For time $t = 1, 2, \dots, T$ do:

Sprinkle N_1 nodes as potential authors uniformly and randomly on a circle S_t^1 (identify each node, e.g. i , by its spatio-temporal coordinates (θ_i, t_i) , where t_i is the generating time of i);

Select N_2 nodes from the new nodes randomly as leaders to attach specific zones: the zone of a leader, e.g. j , is defined as an interval of angular coordinate with center θ_j and length $\alpha(\theta_j)t_j^{-\beta}t^{\beta-1}$ shrinking over time t ,

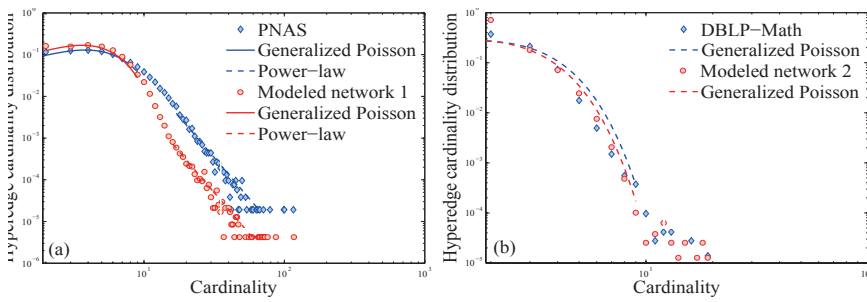


Fig. 2 The distributions of hyperedge cardinalities. Panels show the hyperedge cardinality distributions of two modeled hypergraphs (Parameters of which described in Section 3), PNAS 1999-2013 and DBLP-Math 1956-2013 respectively. The root mean squared errors (RMSE, used for measuring the goodness of fit) are 0.015 (generalized Poisson), 0.002 (power-law) for PNAS. 0.015 (generalized Poisson), 0.002 (power-law) for Modeled network 1, 0.113 for DBLP-Math, and 0.113 for Modeled network 2.

where $\alpha(\theta)$ is a piecewise constant non-negative function of $\theta \in [0, 2\pi)$, and $\beta \in [0.5, 1]$;

2. Connection rules (simply ‘Rule’ hereafter)

For time $t = 1, 2, \dots, T$ do:

(a) For each new node i , search the existing leaders whose zones cover i . For each such leader j , generate a hyperedge with size m by grouping together i , j , and $m - 2$ neighbors of j closest to i , where m is a random variable drawn from $f(x)$ or the number of the neighbors of j plus two if the former is larger than the latter.

(b) Select N_3 existing nodes (no distinction is made between leaders and non-leaders) with non-zero degree randomly, and generate a hyperedge with size m for each selected node l by grouping together l and $m - 1$ randomly selected nodes with the same degree of l , where m is a random variable drawn from $f(x)$ or the number of nodes with the degree of l if the former is larger than the latter.

The leaders are small parts of researchers (potential authors). So N_2 is supposed to be far less than N_1 . Meanwhile, the articles between different research teams are small parts of the total articles, so N_3 is also a small integer. In the description of the model, randomly selecting means sampling without replacement. The sizes of academic impacts and research teams of leaders are imitated by the different sizes of zones. For a leader i , the formula of zonal sizes induces his research team size (the number of the research team members), at time $t > t_i$ is $\delta \alpha(\theta_i) t_i^{-\beta} t^{\beta-1}$, where $\delta = N_1/(2\pi)$. Hence, the cumulative size of the research team is

$$n(\theta_i, t_i, t) = \delta \times \left(\sum_{s=t_i+1}^t \alpha(\theta_i) t_i^{-\beta} s^{\beta-1} \right) \approx \frac{\alpha(\theta_i) \delta}{\beta} \left(\frac{t}{t_i} \right)^\beta. \quad (1)$$

There are some intuitive explanations for the formula of research team sizes $n(\theta_i, t_i, t)$. Firstly, the value of $t - t_i + 1$ is interpreted as the scientific

age of a researcher: a researcher spending more time on research would have a larger academic impact and more collaborators as well, hence it is reasonable to consider the sizes and cumulative sizes of research teams as an increasing function of scientific age, consequently a decreasing function of t_i . Secondly, the cumulative sizes of research teams will increase over t due to the continuously coming collaborators (e.g. tutors may have new students every year). Thirdly, the research team sizes may be different in research topics, so $\alpha(\cdot)$ is introduced to the formula. Finally, Academic impacts of a leader, so the increment of cumulative size of the leader's research team ($\partial^2 n(\theta_i, t_i, t)/\partial t^2 < 0$), could be considered to shrink over time t due to the process of the retirement or activities decrease.

In reality, many article teams are subsets of some research teams, which are often formed by the leaders of research teams and some team members with the similar research interests. This collaboration mode is imitated by Rule (a), which groups together a certain number of nearest nodes and their leader as a hyperedge. Meanwhile, some articles (especially interdisciplinary papers) are unions of some subsets from different research teams. For example, the proportion of the papers marked as interdisciplinary ones in PNAS 1999-2013 is 5.7% [30]. The collaborations between research teams are modeled by Rule (b), which gives a possibility to connect the nodes in different research teams. Following this rule, grouping together certain numbers of nodes with the same degree is the simplest expression of the observed degree assortativity of authors in the empirical data: authors prefer to collaborate with other authors with similar degrees [25]. More reasonable expressions of degree assortativity still need further research.

The parameters of the model can be estimated from the empirical data. For example, the collaborator numbers of authors (the degrees of nodes) in the empirical data are not very large. It means the value of $\alpha(\cdot)$ should be small when N_1 is large. Therefore, the probability of the overlapping of zones is small. So the number of articles generated by Rule (a) is equal to the sum of the number of nodes belonging to a zone (excluding leaders).

Researchers can belong to different research teams at different time. This phenomenon is equivalently imitated by Rule (b) in Step 2 to some extents. In practice, N_3 could be a decimal belonging to the interval $[0, 1]$, which means implementing Rule (b) under probability N_3 at each time step.

3 The data

In order to test the universal reproduction ability of the proposed model, we analyze two empirical coauthorship networks from two metadata with different collaboration levels (Table 1). One is DBLP-Math, which is constructed from 72,269 articles published in 54 mathematical journals during 1956–2013. The article data is obtained from the database DBLP on <http://dblp.uni-trier.de/xml/dblp>. The other one is PNAS, which is constructed from 52,803

articles published in the Proceedings of the National Academy of Sciences (PNAS, <http://www.pnas.org>) during 1999–2013.

In order to analyze the components of authors with large degrees, Sub-PNAS, a sub-network of PNAS, is generated by the articles, the numbers of authors of which are less than 40. The value 40 is the tipping point of the hyperedge cardinality distribution of PNAS 1999–2013, which is detected by the algorithm in Table 2. The inputs are hyperedge cardinalities, $g(\cdot) = \log(\cdot)$ and the PDF of generalized Poisson distribution $h(\cdot) = f_1(\cdot)$.

In the process of extracting networks from those metadata, authors are identified by their names appeared in their articles. It is a reliable way to distinguish authors from one another in most cases. However, it will mistake one author as two if the author changes his/her name in different articles, and two authors as one if they have the same name. Those deficiencies will cause the inaccurate of the empirical network of expressing real coauthorships. Fortunately, the considered statistical properties of those networks show similarities to those of the coauthorship networks with specific operations of author name disambiguation [6, 7]. So using those networks is rational at certain levels.

With properly chosen of model parameters, two synthetic coauthorship networks are generated to reproduce several properties of the empirical data respectively. In detail, for the modeled network 1 (2), $q = 0.9625$ (0.999) in Rule (a), $q = 1$ (0.999) in Rule (b), $f_1(x)$ is the Poisson distribution with mean 5.5 (2.3), and $f_2(x) \propto x^{-3.7}$, $x \in [10, 150]$ ([11, 20]) in Rules (a-b). Set $T = 4, 500$ (9, 000) and $N_1 = 100$ (15) to make the number of nodes comparable to that of the empirical data in magnitude. Set $N_2 = N_1/5$, $\alpha = 0.19$ (0.2) and $\beta = 0.42$ (0.43) to make the average degree comparable to that of the empirical data. Set $N_3 = 1$ (0.5) to make the generated network have a giant component and the node proportion of the giant component comparable to that of the empirical data.

One shortcoming of our model is that in order to make some common features of modelled networks fit those of the empirical data, the input hyperedge cardinality distribution of Modeled network 2 does not fit that of PNAS very well, only captures the features of hook-head and fat-tail.

Table 1 Typical statistic indicators of the analyzed networks.

Network	Nodes	Edges	GCC	AC	AP	MO	PG	NG
PNAS	201,748	1,225,176	0.881	0.230	5.736	0.884	0.868	4,848
DBLP-Math	68,183	99,116	0.756	0.157	9.256	0.935	0.477	15,492
Modeled network 1	193,655	1,261,131	0.788	0.228	5.957	0.952	0.817	6,230
Modeled network 2	70,921	121,685	0.687	0.095	9.429	0.946	0.606	8,940
Sub-PNAS	200,170	1,158,503	0.881	0.097	5.806	0.882	0.867	4,869

The indicators are global clustering coefficient (GCC), assortativity coefficient (AC), average shortest path length (AP), modularity (MO, calculated by the Louvain method [27]), the node proportion of the giant component (PG), and the number of components (NG). The values of AP of the first, third and fifth networks are calculated by sampling.

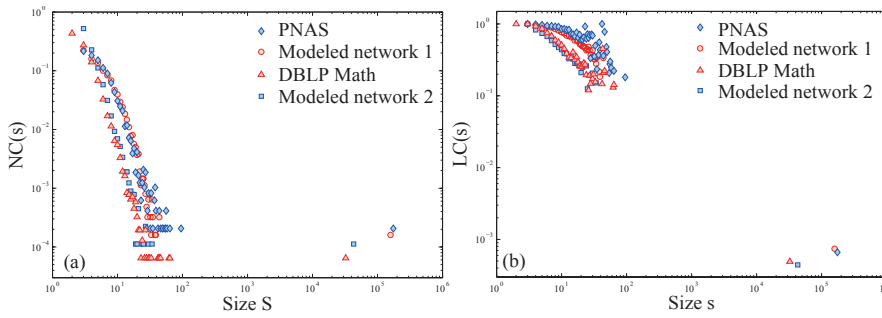


Fig. 3 The distributions of component sizes $NC(s)$ and the average proportion of the largest cliques in s -components (components with size s) $LC(s)$ of the first four networks in Table 1. If there is an s that makes $LC(s) \approx 1$, it means the s -components are nearly fully connected.

The indicator MO in Table 1 shows that the same as the empirical networks, the modeled networks have clear communities. The reason is that the nodes in the same research team probably belong to the same community due to Rule (a) and the connections between research teams are small due to Rule (b). Thus edges within communities are significantly more than those between communities, which results to the clear community structures. The high GCC and small AP show the small world property of the modeled network. In addition, the component size distributions are similar to the empirical data (Fig 3), the reason of which is the same as our previous model in Ref [24], so is omitted here.

4 The components and tipping points of degree distributions

The degree distributions of coauthorship networks (the PDFs of the collaborator numbers of authors) appear two common features, namely hook heads and fat tails, which can be sufficiently fitted by generalized Poisson and power-law distributions respectively. If treating the authors of coauthorship networks as samples, in statistics, such mixture distributions mean those samples come from different populations, namely the collaboration mode of authors with small degrees differs from that with large degrees. In reality, the main part of the authors are the teachers and students in institutes or universities, who can be considered as two populations. The collaboration modes of students and teachers are different: many students only write a few articles, and do not write after graduations, but their teachers could continuously write articles collaborating with their new students or other researchers.

The analytical (Appendix) and numerical evidences (Fig 4) illustrate the ability of our model in reproducing the degree distributions of empirical data. The tunable parameters in the formula of the sizes of influential zones give our model flexibility for empirical networks in different fields. Specifically, the

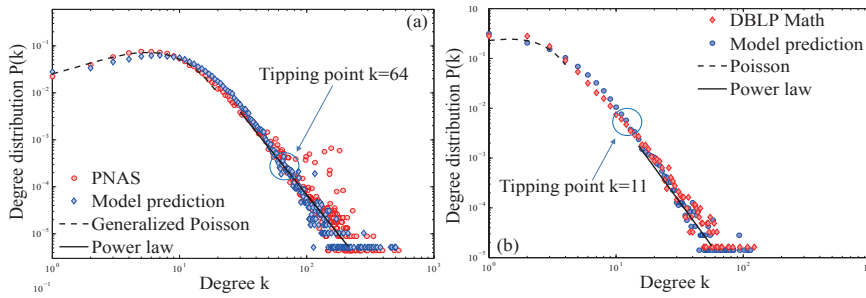


Fig. 4 The degree distributions of the first four networks in Table 1. The fitting functions are the PDFs of generalized Poisson and power-law for the heads and tails respectively. The RMSEs are 0.01 (generalized Poisson), 0.019 (power-law) for PNAS and 0.009 (Poisson), 0.02 (power-law) for DBLP-Math.

power exponents of fat-tails and the hook peaks can be tuned by β and the expected value of f_1 respectively.

There are two essential questions for the emergence of such degree distributions: Why the distributions emerge the Poisson and Power-law; Are there any essential relations between them? We try to give an answer by analyzing and simulating collaboration modes. The event that whether a researcher joins a research team can be treated as a “yes/no” experiment. So the size of a research team is the number of successes in a sequence of n experiments, where n is the number of candidates for the members of the research team. Approximate the probability p of “yes” by its expected value \hat{p} , and suppose those “yes/no” experiments are independent. Then, research team sizes will follow a binomial distribution $B(n, \hat{p})$. When n is large and \hat{p} is small, $B(n, \hat{p})$ can be approximated by a Poisson distribution with mean $n\hat{p}$ (Poisson limit theorem).

In reality, the values of p and n are not constant. Meanwhile, the “yes/no” experiments could be affected by previous occurrences, e.g. students sometimes introduce their research teams to their juniors. So for small research teams, it is reasonable to think their sizes are drawn from a range of generalized Poisson distributions. For large research teams, the number of their candidates are large enough to suppose the “yes/no” experiments are independent. So their sizes could be considered as random variables drawn from a range of Poisson distributions with sufficiently large means. A power-law appears when averaging those Poisson distributions (Eq 4 in Appendix).

Now, we analyze the reason for the emergence of Poisson. The authors with small degrees usually belong to only one small article team (Fig 3a), or come from the small research teams, the sizes of which are less than the mean sizes of article teams. For the first case, the empirical data show that the heads of the distributions of article team sizes are well fitted by generalized Poisson distributions (Fig 2). Hence, the degrees of authors who belong to only one small article team are equal to the size of the article team minus one, hence also follow generalized Poisson distributions. For the second case, authors in those

small research teams probably write articles together. Ignoring the minority of collaborations between research teams, the degrees of those authors are close to the sizes of corresponding research teams minus one, therefore also follow generalized Poisson distributions.

Next, we analyze the reason for the emergence of power-law. The authors with large degrees are the authors of large article teams or the leaders of large research teams. For the first case, the empirical data PNAS shows that large article team sizes follow a power-law distribution with exponent $\gamma = -3.96$ (Fig 2). If supposing each author belongs to only one of such article teams, then the degrees of those authors are drawn from a power-law distribution with exponent $\gamma - 1$. However, the supposition is not fully established in reality (Fig 5b). For the second case, the leaders usually collaborate with all their team members. Ignoring the minority of collaborations between research teams, the degrees of leaders are close to the sizes of corresponding research teams minus one, hence follow a power-law deriving from averaging the Poisson distributions with large means. In fact, the second case illustrates the relation between the Poisson and power-law. It shows that “scale-free”, namely the emergence of power-law tails, partly comes from many Poisson processes, consequently from many “yes/no” experiments. In this sense, coauthorship networks give good examples of “ $1+1>2$ ” for system science and complexity.

At last, we analyze the tipping points of degree distributions from Poisson to power-law. An algorithm is provided to detect those points by using some statistical technologies synthetically (Table 2). Inputs are degrees as observations, $g(\cdot) = \log(\cdot)$ and $h(\cdot) = f_1(\cdot)$. Using $\log(\cdot)$ can rescale the differences between fitting model and empirical data at different scales, which helps to detect the tipping points at small scales.

Table 2 Tipping point detection algorithm for PDFs.

Input: Observations D_s , $s = 1, \dots, n$, rescaling function $g(\cdot)$, fitting model $h(\cdot)$.
For k from 1 to $\max(D_1, \dots, D_n)$ do:
Fit $h(\cdot)$ to the PDF $h_0(\cdot)$ of $\{D_s, s = 1, \dots, n D_s \leq k\}$ by maximum-likelihood estimation;
Do Kolmogorov-Smirnov (KS) test for two data $g(h(t))$ and $g(h_0(t))$, $t = 1, \dots, k$ with the null hypothesis they coming from the same continuous distribution;
Break if the test rejects the null hypothesis at significance level 5%.
Output: The current k as the tipping point.

The tipping-point transition from Poisson to power-law is smooth in DBLP-Math, but nonsmooth in PNAS (Fig 4). A reason for the difference is that the components of large degree nodes in the two data are different. Authors with large degrees in PNAS partly come from large article teams (Fig 5), but DBLP-Math does not have large article teams. If an author only writes articles with small team sizes, the growing process of his/her degree is smooth. In our model, this process is represented by the smooth increasing process of the cumulative sizes of research teams (Eq 1). Meanwhile, the model parameter q

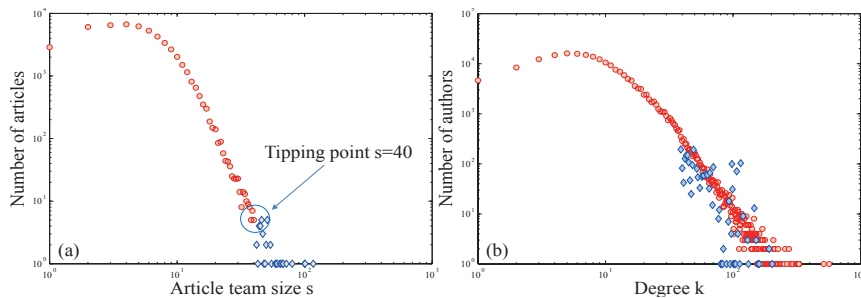


Fig. 5 The components of the authors with many collaborators. Panel (a) shows the article team size distribution and its tipping point (the detecting way of which is described in Section 3) of PNAS 1999-2013. The red circles and blue diamonds in Panel (b) express the degree distributions of the networks extracted from the article teams with sizes $s < 40$ and $s \geq 40$ respectively.

tunes the proportion of large article teams. Hence, when q is very small, the transitions of modeled networks, e.g. Modeled network 2, are smooth.

5 Diversities in clustering behaviour and degree correlation

As global features, the positive Pearson correlation coefficient (PCC) of degree between pairs of collaborated authors (degree assortativity) and high global clustering coefficient (GCC, the fraction of connected triples of nodes which also form “triangles”) are common in coauthorship networks. A general interpretation for degree assortativity for social networks is the homophily of nodes: similar people attract one another [25]. The homophily in research interests of authors can be expressed as article teams. The homophily is also an explanation for high GCC: interattractions between similar people will form a group, in which interconnections between the members could form many triangles.

It can be found that the clustering behaviour and degree correlation differ from the authors with small degrees to those with large degrees. Denote the average local clustering coefficient (LCC) and average degree of neighbors of nodes with degree k by $C(k)$ and $N(k)$ respectively. Degree correlation can be obtained by examining the properties of $N(k)$ [31]. If the function is increasing, nodes with large degrees connect, on average, to nodes with large degrees, which means the network is assortative. Tipping points are detected in those functions (Figs 6,7) by the algorithm in Table 3. The inputs are $C(k)/N(k)$, $g(\cdot) = \log(\cdot)$, and $h(s) = a_1 e^{-((s-b_1)/c_1)^2} / h(s) = a_1 x^3 + a_2 x^2 + a_3 x + a_4$.

When k is larger than the tipping point, the $C(k)$ of each empirical data emerges a decreasing trend, which is proportional to $1/k$. Meanwhile, the PCCs of k and $N(k)$ in two regions of k splitted by tipping points are 0.416/−0.025 and 0.250/−0.046 for PNAS and DBLP-Math respectively. The existence of tipping points in $C(k)$ and $N(k)$ provides an evidence for the difference be-

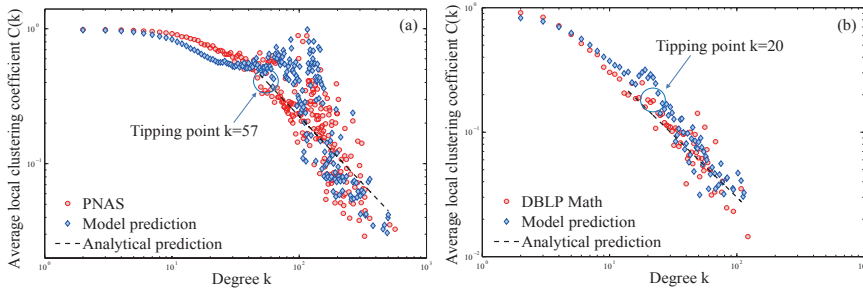


Fig. 6 The relation between local clustering coefficient and degree. The panels show the average local clustering coefficient of k -degree nodes of four networks in Table 1 respectively. The RMSE for the theoretical prediction $C(k) \propto 1/k$ is 0.04597 for PNAS and 0.01476 for DBLP-Math.

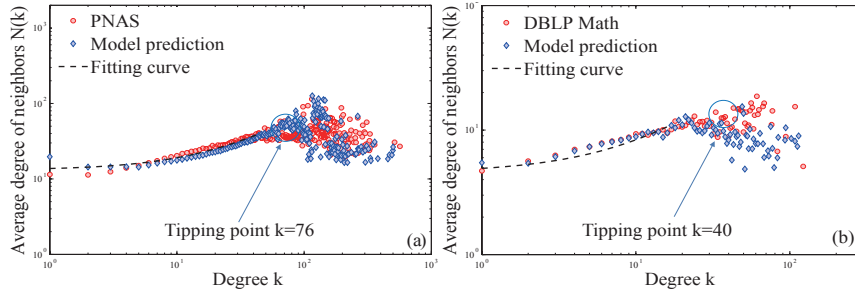


Fig. 7 The relation between degree and average degree of neighbors of nodes. The panels show the average degree of neighbors of nodes with degree k of four networks in Table 1 respectively. The RMSE for the linearly increasing trend is 3.075 for PNAS and 1.313 for DBLP-Math.

tween the collaboration behaviour of authors with small degrees and that of authors with large degrees.

Table 3 Tipping-point detection algorithm for general functions.

Input: Data vector $h_0(s)$, $s = 1, \dots, K$, rescaling function $g(\cdot)$, fitting model $h(\cdot)$
For k from 1 to K do:
Fit $h(\cdot)$ to $h_0(s)$, $s = 1, \dots, k$ by regression;
Do KS test for two data vectors $g(h(s))$ and $g(h_0(s))$, $s = 1, \dots, k$ with the null hypothesis they coming from the same continuous distribution;
Break if the test rejects the null hypothesis at significance level 5%.
Output: The current k as the tipping point.

The low LCCs and non-positive PCC of degree k and $N(k)$ in large k regions cannot be explained by homophily. We try to give an explanation in the following parts. The analysis in Section 4 has illustrated that authors in small research teams (smaller than the mean size of article teams) are more likely to write articles together, and have small degrees on average, because the occurrence probability of collaborations between research teams is small.

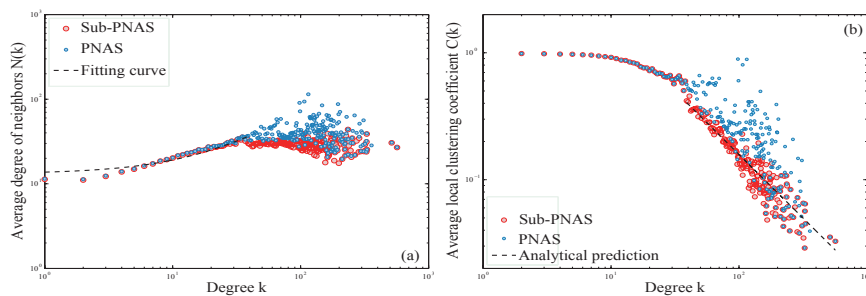


Fig. 8 The influence of large article teams on local clustering coefficients and average degree of node neighbors. The panels show the average local clustering coefficients of nodes with degree k and average degree of neighbors of nodes with degree k of Sub-PNAS and PNAS respectively.

Hence, the authors in a small research team may have high LCCs and similar degrees.

As the cumulative size of a research team increases over time, the degree difference emerges between the leader and non-leaders, because the leader usually collaborates with all members, but non-leaders only write a few articles, the sizes of which are small on average. Teachers and students usually play the roles of leaders and non-leaders respectively, and many students write only a few articles. So the degrees of non-leaders, on average, do not increase with the growth of their leader's degree, which leads to the non-positive PCC of k and $N(k)$ in large k region. Meanwhile, the neighbors of non-leaders probably are non-leaders and in the same article team. So non-leaders have high LCCs, and collaborated non-leaders have similar degrees, which is a reason for positive PCCs of k and $N(k)$ in small k region. In the above analysis, the sizes of articles are approximated by their expected value. However, the existence of large article teams can increase the degree correlation coefficients. For example, the PCCs of k and $N(k)$ in the large k -regions splitted by tipping points are -0.025 and -0.045 for PNAS and Sub-PNAS respectively (Fig 8a). In addition, some non-leaders could leave their team, so are unlikely to collaborate with new coming members. For example, many students leave their research teams after graduations, so the students studied in different periods of time are unlikely to collaborate. The leaving also leads to the low LCC of leaders.

The description in above analysis is imitated in our model. The good fitting of the model to the empirical data confirms the reasonability of the analysis. Especially, the phenomenon of research team members leaving is imitated by shrinking the influential zones, which make some existing non-leaders no longer be the candidates of the new members' collaborators. Only those non-leaders, who are very close to the leader in the sense of geometric distance, could write articles persistently. Above analysis is also partly confirmed by the decreasing trends of the average proportion of the largest cliques in the components with size s (expect the giant) of the empirical data (Fig 3b).

The theoretical analysis and calculation in Appendix show the tails of $C(k)$ of the modeled networks are proportional to $1/k$, which are similar to those of the empirical networks (Fig 6). This law is clear in DBLP-Math, but not so clear in PNAS (Fig 6). The reason is that PNAS has few large article teams, but the theoretical analysis is based on the mean of article team sizes, and ignores large article teams (which occur at low-rates). This reason is confirmed by the clear law in Sub-PNAS, which removes the large article teams (Fig 8b).

The model overcomes two fitting defects of our previous model in Ref [24], namely the $N(k)$ and $C(k)$ of modeled networks are more similar to those of the empirical data. For example, the increasing parts of $N(k)$ here are longer than those of our previous result with the same parameter μ (Fig 5 in Ref [24], Fig 6), a reason of which is described as follows. Suppose node i has an influence zone covers node j . The expected degrees of nodes i and j satisfy $k_i \approx \alpha(\theta_i)\delta t_i^{-\beta}T^\beta/\beta$ and $k_j \leq \mu \log(T/\max(m(\theta_i, t_i), t_j)) + \mu$ respectively. Hence the expected average degree of the neighbors of i is larger than that of our previous model. This also makes the degree associativity of modeled networks do not require a large μ as our previous model does. A small μ makes the $P(k)$ (with a small hook head) and $C(k)$ (with a smooth tipping-point transition) of Modeled network 2 are all similar to those of DBLP-Math (Figs 4b, 6b), and better than those in our previous result (Fig 4 in Ref [24]).

6 Conclusion

A growing geometric graph is proposed to model coauthorship networks with particular concern on tipping-point phenomena of those networks. The model overcomes some shortcomings of our previous model, and provides better predictions of some typical features of the empirical data, e.g. the scaling relation between local clustering coefficient/average degree of neighbors and degree. The model potentially paves a geometric way to understand some aspects of collaboration modes. For example, it explains the emergence of generalized Poisson and Power-law in degree distributions by the different collaboration modes of leaders and other team members of research teams.

Some shortcomings of the model are indicative of the need for further research: The increment of new nodes should not be fixed; New academic leaders could gain more collaborators than old ones; More reasonable expressions are needed for the academic communications between research teams. We are interested in the tipping-point phenomena in citation networks, which are observed and analyzed by G.J. Peterson et al [32]. Is there any relation between the tipping-point phenomena in citation networks and those in coauthorship networks?

References

1. Mali F, Kronegger L, Doreian P, Ferligoj A, Dynamic scientific coauthorship networks (2012) In: Scharnhorst A, Börner K, Besselaar PVD editors. Models of science dynamics. Springer. pp. 195-232.
2. Sarigöl E, Pfitzner R, Scholtes I, Garas A, Schweitzer F (2014) Predicting scientific success based on coauthorship networks. EPJ Data Science 3(1): 1-16.
3. Bertsimas D, Brynjolfsson E, Reichman S, Silberholz JM (2014) Moneyball for academics: Network analysis for predicting research impact. Available at SSRN 2374581.
4. Radicchi F, Castellano C (2015) Understanding the scientific enterprise: citation analysis, data and modeling. In Social Phenomena. Springer pp. 135-151.
5. Newman M (2001) The structure of scientific collaboration networks. Proc Natl Acad Sci USA 98: 404-409.
6. Newman M (2001) Scientific collaboration networks. I. network construction and fundamental results. Phys Rev E 64: 016131.
7. Newman M (2001) Scientific collaboration networks. II. shortest paths, weighted networks, and centrality. Phys Rev E 64: 016132.
8. Newman M (2004) Coauthorship networks and patterns of scientific collaboration. Proc Natl Acad Sci USA 101: 5200-5205.
9. Barabási AL, Jeong H, Néda Z, Ravasz E, Schubert A, Vicsek T. (2002) Evolution of the social network of scientific collaborations. Physica A 311: 590-614.
10. Börner K, Maru JT, Goldstone RL (2004) The simultaneous evolution of author and paper networks. Proc Natl Acad Sci USA 101(suppl 1), 5266-5273.
11. Moody J (2004) The structure of a social science collaboration network: disciplinary cohesion from 1963 to 1999. Am Sociol Rev 69(2): 213-238.
12. Perc C (2010) Growth and structure of Slovenia's scientific collaboration network. J Informetr 4: 475-482.
13. Wagner CS, Leydesdorff L (2005) Network structure, self-organization, and the growth of international collaboration in science. Res Policy 34(10): 1608-1618.
14. Tomassini M, Luthi L (2007) Empirical analysis of the evolution of a scientific collaboration network. Physica A 285: 750-764.
15. Zhou T, Wang BH, Jin YD, He DR, Zhang PP, He Y, et al. (2007) Modeling collaboration networks based on nonlinear preferential attachment. Int J Mod Phys C 18: 297-314.
16. Milojević S (2014) Principles of scientific research team formation and evolution. Proc Natl Acad Sci USA 111: 3984-3989.
17. Catanzaro M, Caldarelli G, Pietronero L (2004) Assortative model for social networks. Phys Rev E 70: 037101.
18. Hoekman J, Frenken K, Tijssen RJW (2010) Research collaboration at a distance: Changing spatial patterns of scientific collaboration within Europe. Res Policy 39: 662-673.
19. Penrose M, *Random geometric graphs*, Oxford studies in probability, 2003.
20. Krioukov D, Kitsak M, Sinkovits RS, Rideout D, Meyer D, Boguñá M (2012) Network cosmology. Sci Rep 2: 793.
21. Xie Z, Ouyang ZZ, Zhang PY, Yi DY, Kong DX (2015) Modeling the citation network by network cosmology. Plos One 10(3): e0120687.
22. Xie Z, Ouyang ZZ, Liu Q, Li JP (2016) A geometric graph model for citation networks of exponentially growing scientific papers. Physica A 456: 167-175.
23. Xie Z, Rogers T (2016) Scale-invariant geometric random graphs. Phys Rev E 93: 032310.
24. Xie Z, Ouyang ZZ, Li JP (2016) A geometric graph model for coauthorship networks. J Informetr 10: 299-311.
25. Newman M (2002) Assortative mixing in networks. Phys Rev Lett 89: 208701.
26. Estrada E, Rodríguez-Velázquez JA (2006) Subgraph centrality and clustering in complex hyper-networks. Physica A 364: 581-594.
27. Blondel VD, Guillaume JL, Lambiotte R, Lefebvre E (2008) Fast unfolding of communities in large networks. J Stat Mech 10: P10008.
28. Newman M, *Networks: an introduction*, Oxford University Press, 2010.

-
29. Consul PC, Jain GC (1973) A generalization of the Poisson distribution. *Technometrics* 15(4): 791-799.
30. Xie Z, Duan XJ, Ouyang ZZ, Zhang PY (2015) Quantitative analysis of the interdisciplinarity of applied mathematics. *Plos One* 10(9): e0137424.
31. Pastor-Satorras R, Vázquez A, Vespignani A (2001) Dynamical and correlation properties of the Internet. *Phys Rev Lett* 87(25): 258701.
32. Peterson GJ, Steve Pressé S, Dill KA (2010) Nonuniversal power law scaling in the probability distribution of scientific citations. *Proc Natl Acad Sci USA* 107: 16023-16027.

7 Appendix

7.1 The underlying formulae of degree distributions

Firstly, we analyze the degree distribution of the network, the edges of which are only generated by Rule (a) in Step 2. The overlapping probability of the zones is small, because $\alpha(\cdot)$ is small (due to the limitation of the maximum degree). Hence the overlapping of zones is ignored in the following analysis. We choose a proper q to make the sizes of the majority of hyperedges be drawn from the Poisson part f_1 with mean $\mu + 1$. We initially consider the effect of those hyperedges on the degree distribution, and next consider that of the hyperedges, the sizes of which are drawn from the power-law part f_2 .

Case 1: the degrees of the nodes having zones. Suppose node i having a zone. Let $S(\theta)$ be the smallest s satisfying $n(\theta, s, T) < \mu$. The expected degree of node i contributed by Rule (a) in Step 2 is $k_a(\theta_i, t_i) \approx n(\theta_i, t_i, T)$ and the approximation holds for $t_i \ll T$. If $S(\theta)$ is large enough (which can be achieved by choosing proper parameters) we have a small $|\partial k_a(\theta_i, s)/\partial s|$ for $s > S(\theta)$, and so we take $k_a(\theta_i, s)$ to be independent of s and write $k_a(\theta_i)$ instead of $k_a(\theta_i, t_i)$.

Case 2: the degrees of the nodes having no zone. Assume node i is covered by a zone of node j . If $S(\theta_j) \leq t_j \leq T$, the expected degree of node i contributed by Rule (a) in Step 2, namely by being covered by the zone of j , is $k_a(t_i, \theta_j, t_j) \approx n(\theta_j, t_j, T) \approx k_a(\theta_j) \approx k_a(\theta_i)$, where the third approximation is due to the small distance $d(\theta_i, \theta_j)$ and the piecewise constant property of $\alpha(\cdot)$. Now we suppose $t_j < S(\theta_j)$. Let $m(\theta_j, t_j)$ be the smallest s satisfying $n(\theta_j, t_j, s) > \mu$ and $k_a(t_i, \theta_j, t_j, s)$ be the expected degree of node i at time s . Since the nodes fall randomly and uniformly, the probability of any existing node in the current influential zone of a leader connecting to a new node is equal. Hence the rate at which node i acquires edges from the nodes coming at time s satisfies

$$\begin{aligned} \partial k_a(t_i, \theta_j, t_j, s)/\partial s &\leq (\mu - 1) \times \alpha(\theta_j) \delta t_j^{-\beta} s^{\beta-1} \times n(\theta_j, t_j, s - 1)^{-1} \\ &\approx \beta(\mu - 1)/s. \end{aligned} \quad (2)$$

Therefore $k_a(t_i, \theta_j, t_j) \leq \beta(\mu - 1) \log(T/\max(m(\theta_j, t_j), t_i)) + \mu$. If t_i is large enough, $k_a(t_i, \theta_j, t_j) \approx \mu$. In addition, $k_a(t_i, \theta_j, t_j) < \beta(\mu - 1) \log(T) + \mu$ so can not effect the tail of the degree distribution.

The degrees of nodes will not be exactly equal to their expected values because the nodes are distributed according to a Poisson point process, and so need to be averaged with the Poisson distribution. In addition, the nodes of the hyperedges with large sizes drawn from f_2 would not have small degrees. Hence the degree distribution of small degree nodes is

$$P_S(k) = \frac{1}{2\pi} \int_0^{2\pi} \left(\frac{\epsilon(\theta) k_a(\theta)^k e^{-k_a(\theta)}}{k!} + \frac{1 - \epsilon(\theta)}{S(\theta) - 1} \sum_{t=1}^{S(\theta)-1} \left(\frac{1}{T - m(\theta, t) + 1} \right. \right. \\ \left. \left. \times \sum_{s=m(\theta, t)}^T \frac{k_a(s, \theta, t)^k e^{-k_a(s, \theta, t)}}{k!} \right) \right) d\theta, \quad (3)$$

where $\epsilon(\theta)$ is the proportion of the nodes covered by the zones of the nodes born on or after time $S(\theta)$. Eq (3) is a mixture of some Poisson distributions with different expected values, namely the expected degree in small regain is not a constant. Meanwhile, the probability of adding a new neighbor for a given node is affected by the spacial locations of previous leaders. Therefore, it is also reasonable to consider that the predominant modeled collaborations are govern by certain generalization of Poisson processes.

The calculation for the degree distribution in large regain is the same as that in Ref [24] and is briefly listed as follows:

$$P_L(k) = \frac{1}{2\pi k!} \int_0^{2\pi} \left(\frac{1}{S(\theta)} \int_1^{S(\theta)+1} k_a(\theta, t, T)^k e^{-k_a(\theta, t, T)} dt \right) d\theta \propto \frac{1}{k^{1+\frac{1}{\beta}}}, \quad (4)$$

where $k \gg 0$ is needed in the calculation. The calculations in Eq 4 are inspired by some of the same general ideas as explored in the cosmological RGGs of Krioukov et al [20].

The hyperedges with large sizes drawn from f_2 can affect the degree distribution tail. Ignoring the overlapping of those hyperedges (which is due to the small probability of their occurrences) and the proportion of the nodes having zones and belonging to those hyperedges (which is small when compared with that of the nodes having no zone) we obtain that the degree distribution tail of the network generated by Rule (a) in Step 2 is approximately a mixture power-law distribution $qP_L(k) + (1 - q)(k + 1)f_2(k + 1)/\sum_s s f_2(s)$.

Finally, we analyze the degrees contributed by Rule (b). Let $k_b(\theta_i, t_i, s)$ be the degree of node i contributed by this rule at time $s \geq t_i$. The number of nodes with nonzero degree at time s is $N(s) = \zeta \int_0^{2\pi} (\sum_{t=1}^s \alpha(\theta) \delta t^{-\beta} s^\beta / \beta) d\theta \approx s \delta \zeta \int_0^{2\pi} \alpha(\theta) d\theta / (\beta(1 - \beta))$, where $\zeta = N_2 / (2\pi)$. So the probability that a node is chosen by Rule (b) in Step 2 at time s is $(\nu + 1)N_3 / N(s)$, where $\nu + 1$ is the expected value of f in Rule (b) in Step 2. Hence, the rate at which node i at time s acquires edges generated by Rule (b) is $\partial k_b(t_i, s) / \partial s = \nu(\nu + 1)N_3 / N(s)$, which gives $k_b(t_i, T) \approx \beta(1 - \beta)\nu(\nu + 1) \log(T/t_i)N_3 / (\delta \zeta \int_0^{2\pi} \alpha(\theta) d\theta)$. Hence, choosing proper parameters, the degrees contributed by Rule (b) can be ignored, when compared with that contributed by Rule (a) in Step 2.

In simulations, the condition $k \gg 0$ required in Eq (4) can not be fully satisfied due to the restriction of the maximum degree, which is a reason for the difference between the theoretical value and the practical value of the power exponent. However, the degree distributions of the modeled networks fit the above analysis at certain levels, and are similar to those of the empirical networks respectively (Fig 4).

7.2 The underlying formulae of the correlation of local clustering coefficients and degrees

Suppose node i has a zone and t_i is small enough. So the number of neighbors of node i generated by Rule (b) in Step 2 can be ignored compared with that generated by Rule (a) in Step 2. Hence the expected degree k of i is approximately equal to $k_a(\theta_i, t_i, T)$. Suppose nodes j, l belong to the zone and $t_j < t_l$. Since t_i is small, k is large, so $T - m(\theta_i, t_i) \approx T - T(\mu/k)^{1/\beta} \approx T$, where $m(\theta_i, t_i)$ is the smallest s satisfying $n(\theta_i, t_i, s) > \mu$. So we can only consider the case $t_j > m(\theta_i, t_i)$. Since the nodes are dropped randomly and uniformly, the probability of an edge between j and l is $\omega T^\beta / (k(t_l - 1)^\beta)$ the reciprocal of the number of nodes (born before t_l) of the zone multiplied by ω , the expected hyperedge size less than two, where the boundary effects of zones are ignored. Averaging over possible values of t_j and t_l , the LCC of node i is

$$\begin{aligned} C(k) &= \frac{1}{T - m(\theta_i, t_i)} \int_{m(\theta_i, t_i)}^T \left(\frac{1}{T - t_j - 1} \int_{t_j+1}^T \frac{\omega T^\beta}{k(t_l - 1)^\beta} dt_l \right) dt_j \\ &\approx \frac{\omega T^{\beta-1}}{k(1-\beta)} \left(\int_{m(\theta_i, t_i)}^T \frac{(T-1)^{1-\beta} - s^{1-\beta}}{T-s-1} ds \right), \end{aligned} \quad (5)$$

where the approximation holds for $T \gg m(\theta_i, t_i)$. Denote the coefficient of $1/k$ by $I(k)$, substitute $m(\theta_i, t_i) \approx T(\mu/k)^{1/\beta}$ into it, and differentiate it to obtain

$$\frac{dI(k)}{dk} = \frac{\omega T^{\beta-1}}{1-\beta} \times \frac{(T-1)^{1-\beta} - T^{1-\beta} \left(\frac{\mu}{k}\right)^{\frac{1-\beta}{\beta}}}{T - T \left(\frac{\mu}{k}\right)^{\frac{1}{\beta}} - 1} \times \frac{T}{\beta} \frac{\mu^{\frac{1}{\beta}}}{k^{\frac{1}{\beta}+1}} \approx \frac{\omega \mu^{\frac{1}{\beta}}}{\beta(1-\beta)k^{\frac{1}{\beta}+1}}, \quad (6)$$

which is approximately equal to 0 if $k \gg \mu$. Hence $I(k)$ is free of k and $C(k) \propto 1/k$ if k is large enough. The modeled networks roughly follow the above analyses (Blue diamonds in Fig 6), in which the outliers are partly caused by the boundary effects of zones that can not be ignored under the occurrence of some large size hyperedges drawn from $f_2(x)$.